

---

**ELECTRODYNAMICS  
AND WAVE PROPAGATION**

---

# The Spectrum of Whispering-Gallery Modes with Large Azimuthal Indexes in Thin Disk Dielectric Resonators

**B. M. Garin, V. P. Mal'tsev, V. V. Meriakri, B. A. Murmuzhev,  
M. P. Parkhomenko, and N. A. Fedoseev**

Received August 19, 2004

**Abstract**—The dispersion and resonance characteristics of whispering-gallery modes in a resonator with a small height-to-radius ratio are investigated theoretically and experimentally. It is shown that the calculated mode frequencies and azimuthal indexes match the experimental data obtained in the millimeter-wave range for resonators fabricated from certain materials. A maximum is revealed in the dependence of frequency intervals between neighboring modes on the azimuthal index at large values of the latter.

PACS numbers: 41.20.Jb, 77.84.-s

DOI: 10.1134/S1064226908030054

## INTRODUCTION

High- $Q$  disk dielectric resonators (DDR) are used for frequency stabilization in microwave oscillators, resonance filters, etc. [1]. In spectroscopy, such resonators are applied for measurements of dielectric loss in the material of a resonator [2–4]. Determination of attainable low dielectric loss in the material of a DDR is limited by its finite radiation  $Q$  factor [5], which grows with the radius of the disk [6, 7]. A DDR with a large radius may support higher-order modes with a large number (azimuthal index  $n$ ) of field variations along the disk's perimeter. The energy of such waves concentrates mainly near the cylindrical surface of the disk. By analogy with the corresponding acoustic waves, the aforementioned waves are called whispering-gallery modes (WGMs) [8].

The increase of the azimuthal index observed when a DDR's radius or the frequency grows leads to an increase in the number of resonance curves in the WGM frequency spectrum. As a result, frequency overlapping of the resonance curves of WGMs with close azimuthal indexes may occur. In this case, the electromagnetic interaction between WGMs may develop and, as a consequence, the shapes, amplitudes, and widths of resonance curves may be distorted. As a result, the actual  $Q$  factor of a DDR is measured with a large error. Therefore, measurements of extremely low dielectric loss may be limited by an increase in the mode spectral density (the number of modes and resonance curves in a fixed frequency band) at a large radius of a disk. In this context, it is of interest to analyze the distribution of WGM frequencies at large values of a resonator's radius and of the

azimuthal index, in particular, in the region of strong dispersion of the slowing effect [9].

There are various analytic methods [10–13] for calculation of dispersion equations (DEs) for waves propagating in DDRs. These methods include approximate methods of partial domains [10, 11, 13] and magnetic walls [11] and the method of effective permittivity (EP) [14]. As compared to other methods, the latter method yields results that are more accurate. In the EP method, the 3D problem of solution of the DE for waves in a DDR is reduced to two 2D problems: (i) for a dielectric cylinder that has the same radius as the DDR and is infinite along the  $z$  axis and (ii) for a plane plate (PP) that is characterized by the EP, has a height equal to the  $z$  height of the disk, and is infinite in the transverse direction.

The purpose of this study is to develop a method for calculation of the resonance frequencies of hybrid WGMs propagating in a DDR and to numerically analyze their spectral characteristics at large azimuthal indexes. Most attention is focused on the investigation of the dependence of WGM frequencies on the azimuthal index and on the dielectric and geometric parameters of a DDR.

## 1. THE DISPERSION PROPERTIES OF HYBRID WGMs IN A DIELECTRIC CYLINDER

According to the EP method, it is necessary to analyze the dispersion characteristics (DCs) of WGMs in a dielectric cylinder.

A generalized DE for hybrid waves propagating in a circular dielectric cylinder infinite along the  $z$  axis was

derived for the first time in [15]. In terms of reduced parameters, this DE has the following form [16]:

$$\left[ \frac{\varepsilon_1 J'_n(\beta)}{\beta J_n(\beta)} + \frac{K'_n(\alpha)}{\alpha K_n(\alpha)} \right] \left[ \frac{\mu_1 J'_n(\beta)}{\beta J_n(\beta)} + \frac{K'_n(\alpha)}{\alpha K_n(\alpha)} \right] = n^2(\alpha^{-2} + \beta^{-2})(\varepsilon_1 \mu_1 \beta^{-2} + \alpha^{-2}), \quad (1)$$

where  $n$  is the azimuthal index;  $J_n(\beta)$  is the Bessel function of the first kind;  $K_n(\alpha)$  is the  $n$ th-order Macdonald function;  $\beta = k_{\perp 1} r_1$  and  $\alpha = k_{\perp 2} r_1$  are the internal and external reduced transverse wave numbers, respectively;  $k_{\perp 1}$  and  $k_{\perp 2}$  are the internal and external transverse wave numbers, respectively;  $r_1$  is the radius of the dielectric cylinder; and  $\varepsilon_1$  and  $\mu_1$  are the relative permittivity and permeability of the dielectric cylinder, respectively. It is assumed that, outside the cylinder, the permittivity is  $\varepsilon_2 = 1$  and the permeability is  $\mu_2 = 1$ . Reduced wave numbers  $\alpha$  and  $\beta$  are coupled through the additional relationships [16]

$$\alpha^2 + \beta^2 = R^2, \quad \gamma^2 = (k_0 r_1)^2 \varepsilon_1 - \beta^2, \quad (2)$$

$$\gamma^2 = (k_0 r_1)^2 \varepsilon_2 + \alpha^2,$$

where  $R = F \sqrt{\varepsilon_1 - \varepsilon_2}$ ,  $F = k_0 r_1 = (2\pi/\lambda_0)r_1 = (2\pi f r_1/c) = (\omega r_1/c)$  is the reduced (dimensionless) frequency;  $\lambda_0$  and  $k_0$  are the wavelength and wave number in free space, respectively;  $\gamma$  is the dimensionless constant of wave propagation along the  $z$  axis; and  $c$  is the velocity of light in free space.

It is seen that, when  $n \neq 0$ , DE (1) cannot be split into independent equations for electric ( $H_z = 0$ , the first square brackets) TE waves and magnetic ( $E_z = 0$ , the second square brackets) TM waves. Therefore, when  $n \neq 0$ , WGMs are hybrid TEM waves and have all of the six components of the electromagnetic field.

In studies [6, 10], calculations at  $\gamma \rightarrow 0$  are simplified through conventional division of hybrid WGMs into TE and TM modes [17], each having three components:  $H_z$ ,  $E_\rho$ , and  $E_\phi$  in a TE mode  $E_z$ ,  $H_\rho$ , and  $H_\phi$  in a TM mode. Evidently, owing to this conventional division, the accuracy of computed WGM DCs is deteriorated at  $\gamma \neq 0$ . Therefore, in this study, we propose a method of direct solution of DE (1) (the vector problem) for hybrid WGMs with large  $n$ .

In order to simplify solution of DE (1), let us use recurrence relationships [18] for derivatives  $J'_n(\beta)$  and  $K'_n(\alpha)$  of the Bessel and Macdonald functions and introduce the new dimensionless parameter  $M = \alpha/\beta$ . With the new dimensionless parameters, reduced trans-

verse wave numbers  $\alpha$  and  $\beta$  and propagation constant  $\gamma$  are determined as follows:

$$\alpha = MR/\sqrt{1 + M^2}, \quad \beta = R/\sqrt{1 + M^2}, \quad (3)$$

$$\gamma/F = \sqrt{(\varepsilon_1 M^2 + \varepsilon_2)/(1 + M^2)} \equiv \sqrt{\varepsilon_{\text{ef}}}, \quad (4)$$

where  $\gamma/F$  is the relative slowing parameter and  $\varepsilon_{\text{ef}}$  is the effective permittivity.

With allowance for expressions (2) and (3), DE (1) is modified into the form

$$M^2 R^2 \{ \varepsilon_1 M K_n(\alpha) [J_{n-1}(\beta) - J_{n+1}(\beta)] - J_n(\beta) [K_{n-1}(\alpha) + K_{n+1}(\alpha)] \} \times \{ \mu_1 M K_n(\alpha) [J_{n-1}(\beta) - J_{n+1}(\beta)] - J_n(\beta) [K_{n-1}(\alpha) + K_{n+1}(\alpha)] \} \quad (5)$$

$$- 4J_n^2(\beta) K_n^2(\alpha) n^2 (1 + M^2) (1 + \varepsilon_1 \mu_1 M^2) = 0.$$

Equation (5) characterizes the complex functional relationship of parameters  $R$  and  $n$  with parameter  $M$ . According to formula (4), the relative slowing parameter is expressed through parameter  $M$ . When permittivity  $\varepsilon_1$  and permeability  $\mu_1$  are known and quantities  $n$  and  $M$  are specified, parameter  $R$  is determined from solution of DE (5).

Obviously, DE (5) has a solution when parameters  $M$  and  $R$  range within the intervals  $0 \leq M < \infty$  and  $0 \leq R < \infty$ . At  $M = 0$  ( $\gamma/F = \sqrt{\varepsilon_2}$ ,  $\alpha = 0$ ), the cutoff of WGM propagation occurs and, for  $n \neq 0$ , there exist critical cutoff frequencies, i.e., specific values  $R = R_0$ , where  $R_0$  is the reduced critical cutoff frequency. In this case, the Macdonald function in DE (5) [18] has the form

$$K_n(\alpha) = \frac{1}{2} \Gamma(n) \left( \frac{2}{\alpha} \right)^n, \quad (6)$$

where  $\Gamma$  is the gamma function.

At  $\alpha = 0$ , we have  $M = 0$ . In this case, function  $K_n(\alpha)$  tends toward infinity, the transverse wave number takes the value  $\beta = R_0$ , and we find from DE (5) that

$$J_n(R_0) = 0. \quad (7)$$

Note that Eq. (7) coincides with the condition for the cutoff of propagation of electric WGMs [17].

In another limiting case, when  $M \gg 1$ , we have  $\alpha \rightarrow R$  and  $\beta \rightarrow R/M$  for the transverse wave numbers and  $\gamma/F \rightarrow \sqrt{\varepsilon_1}$  for the slowing parameter. In this case, the Macdonald functions satisfy the relationship

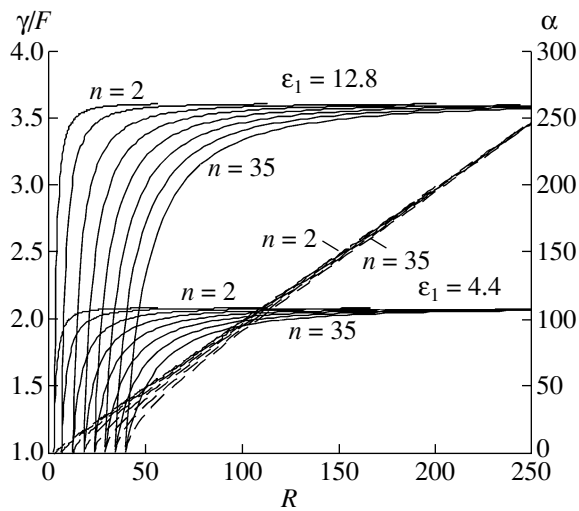


**Fig. 1.** Dispersion characteristics of hybrid WGMs in a dielectric cylinder obtained at various values of permittivity  $\epsilon_1$  and azimuthal index  $n$ .

$K_n(\alpha) \approx \exp(-\alpha) \ll 1$  [18]. Then,  $K_{n-1}(\alpha) \approx K_n(\alpha) \approx K_{n+1}(\alpha)$  and DE (5) can be modified as follows:

$$R^2 \{ \epsilon_1 M [J_{n-1}(\beta) - J_{n+1}(\beta)] - 2J_n(\beta) \} \times \{ \mu_1 M [J_{n-1}(\beta) - J_{n+1}(\beta)] - 2J_n(\beta) \} - 4J_n^2(\beta) n^2 \epsilon_1 \mu_1 M^2 = 0. \quad (8)$$

It follows from DE (8) that, when  $n \gg 1$  and

$$J_{n-1}(\beta) - J_{n+1}(\beta) \approx 0, \quad (9)$$

parameter  $R$  satisfies the relationship  $R \approx nM \sqrt{\epsilon_1 \mu_1} \gg 1$ , which corresponds to propagation of magnetic-type electromagnetic waves in a dielectric cylinder [17].

When  $n \gg 1$ , the WGM energy concentrates mainly near the surface of the dielectric cylinder. Therefore, function  $J_n(\beta)$ , which characterizes the radial distribution of WGM fields, reaches its maximum near this surface when  $\beta < \beta_1$ , where  $\beta_1$  is the first ( $m = 1$ ) root of the function  $J_n(\beta)$  [18]. Hence, it suffices to determine only the first root of DE (5). This situation corresponds to propagation of hybrid  $TEM_{1n}$  WGMs in the dielectric cylinder.

The DCs of hybrid  $TEM_{1n}$  WGMs propagating in the dielectric cylinder have been calculated at frequencies of about 100 GHz and the fixed azimuthal indexes  $n = 2, 5, 10, 15, 20, 25, 30,$  and  $35$  for weakly absorbing dielectrics (fluoroplastic,  $\epsilon_1 = 2.08$ ; fused quartz,  $\epsilon_1 = 4.4$ ; diamond,  $\epsilon_1 = 5.7$ ; alumina,  $\epsilon_1 = 9.8$ ; silicon,  $\epsilon_1 = 11.6$ ; and gallium arsenide,  $\epsilon_1 = 12.8$ ) with the dielectric loss  $\tan \delta < 10^{-3}$ . The DCs of hybrid  $TEM_{1n}$  WGMs propagating in gallium arsenide and fused-quartz dielectric cylinders are depicted in Fig. 1. The solid

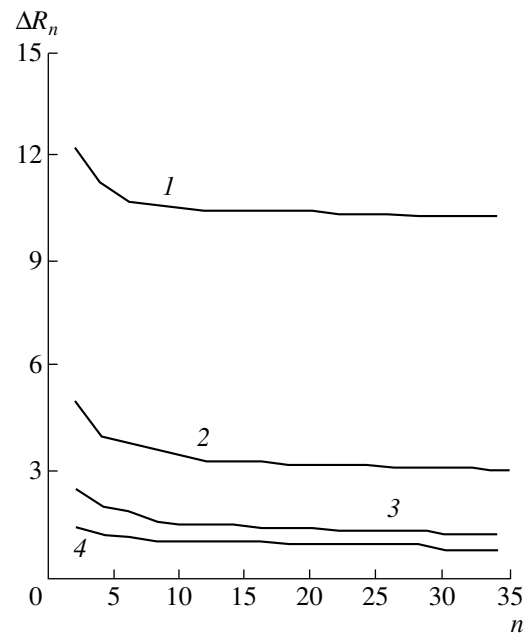


**Fig. 2.** Frequency intervals between neighboring WGMs in a quartz dielectric cylinder: Curves 1–4 correspond to  $\gamma/F = 2.1, 2.0, 1.5,$  and  $1.0$ , respectively.

curves characterize the dependence of the slowing parameter  $\gamma/F$  on  $R$ . The dashed curves show reduced external wave number  $\alpha$  as a function of  $R$ . All the curves are arranged top-down in the ascending order of  $n$ :  $n = 2, \dots, 35$ .

It is of interest to analyze the rarefaction of the spectrum of the DCs, i.e., the dependences  $\Delta R_n \equiv R_{n+1} - R_n$  on azimuthal index  $n$  at constant  $\gamma/F$ , where  $R_n$  is the frequency parameter of the mode with index  $n$ . These curves correspond to the horizontal sections in Fig. 1. Evidently, the increasing crowding of the curves corresponds to the growth of modes with different azimuthal indexes  $n$  in the given range of parameter  $R$ . This effect should lead to a decrease in  $\Delta R_n$ .

Figure 2 shows the dependences of  $\Delta R_n$  on  $n$  that are obtained from the horizontal sections of the DCs (Fig. 1) for fused quartz ( $\epsilon_1 = 4.4, \epsilon_2 = 1$ ). It is seen that, as azimuthal index  $n$  grows, the curves crowd. This effect corresponds to a decrease in quantity  $\Delta R_n$ . This quantity exhibits the maximum variation  $\Delta R_n$  in the interval  $1 < n < 10$ . At larger  $n$ , these curves reach the horizontal sections corresponding to the conditions  $\Delta R_n \approx a$ , where  $a$  is constant for each value of  $\gamma/F$ . As  $\gamma/F$  grows,  $a$  increases. This increase corresponds to a larger frequency spacing between the DCs.

When  $n > 10$ , the dependence (calculated from formula (9)) of  $\Delta R_n$  on  $n$  coincides with curve 1 from Fig. 2. This circumstance means that, at large slowing param-

eters when  $\gamma/F \approx \sqrt{\epsilon_1}$ , hybrid WGMs are transformed into magnetic WGMs.

Note the following fundamentally important result of our investigations: As azimuthal index  $n$  grows, frequency rarefaction  $\Delta R_n$  of the spectrum of WGMs in a dielectric cylinder tends toward a constant that increases with the slowing parameter. Electric WGMs ( $H_z = 0$ , at  $\gamma F \approx \sqrt{\epsilon_2}$ ) are transformed into hybrid waves ( $E_z \neq 0, H_z \neq 0$ ), which exist when  $\sqrt{\epsilon_2} < \gamma F < \sqrt{\epsilon_1}$ . Hybrid WGMs are transformed into magnetic waves ( $E_z = 0$ ) at  $\gamma F \approx \sqrt{\epsilon_1}$ .

## 2. THE DISPERSIVE PROPERTIES OF WAVES IN A PLANE PLATE

It is assumed that a transversely infinite PP of finite height  $2b_1$  has permittivity  $\epsilon_{ef}$  that is determined from expression (4). Let us introduce the cylindrical coordinate frame whose  $z$  axis is perpendicular to the PP, while the  $r$  and  $\phi$  coordinates lie in the PP plane. In this case, according to [17], the electromagnetic fields in the PP can be expressed in terms of two potential functions  $\Psi_h$  and  $\Psi_e$ :

$$\begin{aligned}
 E_r &= -ik_0\mu \frac{1}{r} \frac{\partial \Psi_h}{\partial \phi} + \frac{\partial^2 \Psi_e}{\partial z \partial r}, & E_\phi &= ik_0\mu \frac{\partial \Psi_h}{\partial r} + \frac{1}{r} \frac{\partial^2 \Psi_e}{\partial z \partial \phi}, \\
 E_z &= k_\perp^2 \Psi_e, \\
 H_r &= ik_0\epsilon \frac{1}{r} \frac{\partial \Psi_e}{\partial \phi} + \frac{\partial^2 \Psi_h}{\partial z \partial r}, \\
 H_\phi &= -ik_0\epsilon \frac{\partial \Psi_e}{\partial r} + \frac{1}{r} \frac{\partial^2 \Psi_h}{\partial z \partial \phi}, & H_z &= k_\perp^2 \Psi_h.
 \end{aligned}
 \tag{10}$$

Potential functions  $\Psi_{e,h}$  in expressions (10) are chosen with allowance for the geometry of the problem from the condition that there is no field at an infinitely large distance from the PP planes. Let hybrid cylindrical waves propagating in the PP be, simultaneously, standing along the  $z$  axis and traveling in the transverse direction. Then,

$$\begin{aligned}
 \Psi_e &= [A_1 \sin(\gamma_1^e z) + B_1 \cos(\gamma_1^e z)] \\
 &\times H_n^{(2)}(k_\perp^e r) \cos(n\phi),
 \end{aligned}
 \tag{11}$$

$$\Psi_h = [C_1 \sin(\gamma_1^h z) + D_1 \cos(\gamma_1^h z)] H_n^{(2)}(k_\perp^h r) \sin(n\phi)$$

in the interior of the PP and

$$\begin{aligned}
 \Psi_e &= F_2^\mp \exp[\mp \gamma_2^e(z \pm b_1)] H_n^{(2)}(k_\perp^e r) \cos(n\phi), \\
 \Psi_h &= G_2^\mp \exp[\mp \gamma_2^h(z \pm b_1)] H_n^{(2)}(k_\perp^h r) \sin(n\phi)
 \end{aligned}
 \tag{12}$$

in the exterior of the PP, where  $A_1, B_1, C_1, D_1, F_2^\mp$ , and  $G_2^\mp$  are the wave amplitudes,  $\gamma_{1,2}^{e,h}$  are the longitudinal wave numbers in the interior and exterior of the plate,  $k_\perp^{e,h}$  are the propagation constants of the cylindrical wave, and  $H_n^{(2)}(k_\perp^{e,h} r)$  is the Hankel function of the second kind. The plus and minus signs refer to the interfaces on the PP planes at  $z = +b_1$  and  $-b_1$ , respectively.

The boundary conditions for the continuity of the tangential field components on the PP surfaces at  $z = \pm b_1$  yield a system of linear algebraic equations for amplitudes  $A_1, B_1, C_1, D_1, F_2^\mp$ , and  $G_2^\mp$ . The consistency of these equations yields

$$\begin{aligned}
 N_{e,h} &= \frac{1}{\kappa} \\
 &\times \begin{cases} \tan(A_1^{e,h}/\sqrt{1+N_{e,h}^2}) & \text{for odd modes} \\ -\cot(A_1^{e,h}/\sqrt{1+N_{e,h}^2}) & \text{for even modes,} \end{cases}
 \end{aligned}
 \tag{13}$$

where  $\kappa = \epsilon_{ef}/\epsilon_2$  for electric TE cylindrical waves in the PP,  $\kappa = \mu_1/\mu_2$  for magnetic TM waves,  $N_{e,h} = \gamma_2^{e,h}/\gamma_1^{e,h}$ , and  $A_1^{e,h} = k_0 b_1 \sqrt{\epsilon_{ef} - 1}$ .

It is seen from DE (13) that hybrid cylindrical waves propagating in a PP with an infinite transverse dimension ( $r \rightarrow \infty$ ) are divided into electric TE and magnetic TM modes.

Longitudinal wave numbers  $\gamma_{1,2}^{e,h}$  are expressed through reduced parameters  $A_1^{e,h}$  and  $N_{e,h}$ :

$$\begin{aligned}
 \gamma_1^{e,h} b_1 &= A_1^{e,h} / \sqrt{1 + N_{e,h}^2}, \\
 \gamma_2^{e,h} b_1 &= A_1^{e,h} N_{e,h} / \sqrt{1 + N_{e,h}^2}.
 \end{aligned}
 \tag{14}$$

The relative propagation constant of cylindrical waves in the PP is determined from the expression

$$\beta_{e,h} = \frac{k_\perp^{e,h} r_1}{F} = \sqrt{\frac{(\epsilon_1 M^2 + \epsilon_2) N_{e,h}^2 + \epsilon_2 (1 + M^2)}{(1 + M^2)(1 + N_{e,h}^2)}}.
 \tag{15}$$

Dispersion equations (5) and (13) are functionally coupled through effective permittivity  $\epsilon_{ef}$  and the normalization of the parameters:

$$\begin{aligned}
 \gamma_{1,2}^{e,h} b_1 &= \gamma_{1,2}^{e,h} t r_1, & A_1^{e,h} &= t F \sqrt{\epsilon_{ef} - 1}, \\
 & & t &= b_1 / r_1.
 \end{aligned}
 \tag{16}$$

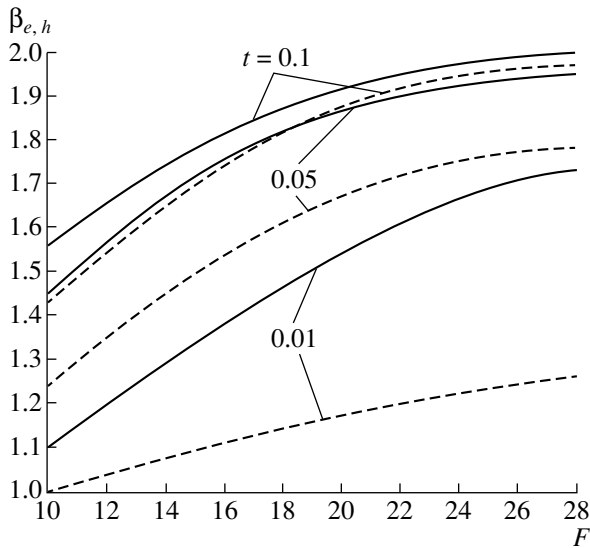


**Fig. 3.** Dispersion characteristics of TE and TM WGMs in a DDR obtained at various values of  $t$ .

The DCs of TE (solid curves) and TM (dashed curves) cylindrical waves propagating in a PP with the permittivity  $\epsilon_1 \approx 5.7$  (diamond) and  $t \equiv b_1/r_1 = 0.01, 0.05, \text{ and } 0.10$  are depicted in Fig. 3 for the particular case  $n = 10$ . It is seen that small values of  $t$  substantially affect the DCs. When  $t > 0.1$ , the curves for TE and TM waves degenerate.

As the PP's permittivity grows, the steepness of the DCs increases and, at each value of  $t$ , the difference between the slowing parameters of TE and TM waves decreases. At higher values of azimuthal index  $n$ , the DCs shift toward larger reduced frequency  $F$ .

### 3. THE RESONANCE FREQUENCIES OF DDRs

The resonance frequencies of DDRs are determined from the consistent solution of DEs (5) and (13) under the condition that  $\beta_{e,h} = k_{\perp}^{e,h}$ . Equation (13) can be modified into the form

$$\kappa \gamma_2^{e,h} = \gamma_1^{e,h} \begin{cases} \tan(t\gamma_1^{e,h}) \\ -\cot(t\gamma_1^{e,h}), \end{cases} \quad (17)$$

where  $\gamma_1^{e,h} = [F_d^2 \epsilon_1 - F_c^2 (\epsilon_1 - \epsilon_2) + \alpha^2]^{1/2}$ ,  $\gamma_2^{e,h} = [F_c^2 (\epsilon_1 - \epsilon_2) - \alpha^2 - F_d^2 \epsilon_2]^{1/2}$ , and  $\kappa = \epsilon_{ef}/\epsilon_2$ . The indices "c" and "d" refer to the reduced resonance wave numbers of the cylinder and DDR, respectively.

The dependences of  $R/\sqrt{(\epsilon_1 - \epsilon_2)} = F_c$  on azimuthal index  $n$  are determined from the calculated DCs (Fig. 2) corresponding to a solution to Eq. (5) for a dielectric cylinder with given  $\epsilon_1$  and  $\epsilon_2$ . For specified values of

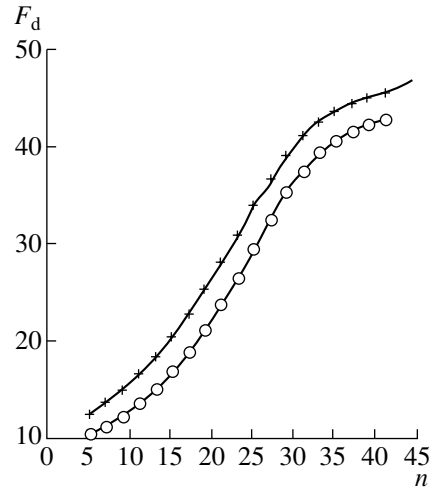


**Fig. 4.** Dependence of reduced frequencies  $F_d$  of WGMs in a diamond DDR on  $n$ :  $t \equiv b/r_1 =$  (circles) 0.01 and (crosses) 0.10.

$\gamma/F = \sqrt{\epsilon_{ef}}$ ,  $F_c$ , and  $\alpha$ , the functional relationship between  $F_d$  and index  $n$  is determined from DE (17). The resonance frequencies of WGMs in the DDR correspond to the intersection points of the curves for the aforementioned dependences at  $F_c = F_d$ .

Figure 4 shows the dependences of WGM reduced resonance frequency  $F_d$  on azimuthal index  $n$  for a diamond ( $\epsilon_1 = 5.7$ ) DDR with the section formats  $t = 0.01$  (circles) and 0.10 (crosses). It is seen that, at constant  $n$  (vertical sections in Fig. 4),  $F_d$  increases with  $c$ . This circumstance is due to the fact that, in a DDR of a large height, the slowing parameter and frequencies of WGMs increase.

The dependence of intervals  $\Delta F_d$  between WGM frequencies on index  $n$  can easily be found from Fig. 4. This dependence is shown in Fig. 5. It is seen that, at certain large  $n$ , quantity  $\Delta F_d$  reaches its maximum. This effect can be explained qualitatively by a change in the distributions of the electromagnetic fields in the interior and exterior of the DDR. At small  $n$  and low frequencies (small  $F_d$ ), the external wave number satisfies the inequality  $\alpha < 1$  and, according to expression (10), the field intensities in the exterior of the DDR are rather high. In this case,  $\epsilon_{ef} \approx \epsilon_2$  and the propagation of WGMs is similar to the propagation of cylindrical waves in an infinite medium.

The values of WGM reduced frequencies  $F_d$  and of wave number  $\alpha$  increase with  $n$ . As a result, the fields in the interior and exterior of the DDR are redistributed. According to the functional dependence  $J_n(\beta)$  [18], the maximum WGM field shifts to the cylindrical surface and the field in the exterior of the DDR

exponentially decreases. In this case,  $\epsilon_2 < \epsilon_{ef} < \epsilon_1$ , and the dispersive properties of WGMs are substantially affected by the boundary conditions on the cylindrical and lateral surfaces of the DDR. An evident result is strong dispersion and, as a consequence, the maximum rarefaction of the frequency spectrum of WGMs in the DDR. While  $n$  continues to grow,  $F_d$  increases, the external transverse wave number satisfies the inequality  $\alpha \gg 1$ , and the fields in the exterior of the DDR are negligibly small. The field in the interior of the DDR reaches its maximum near the cylindrical surface and practically vanishes in the center region of the DDR. In this case, the DDR is similar to a ring resonator, where crowding of the spectrum of WGM frequencies, i.e., a decrease in  $\Delta F_d$ , is observed as WGM frequencies grow.

If the spectrum of WGM frequencies is known, azimuthal index  $n$  for each resonance frequency can be determined approximately from the condition  $J'_n(x) = 0$ , where  $x = k_0 r_1 \sqrt{\epsilon_1}$ . For  $x > n$ , the higher order Bessel functions can be calculated from the asymptotic representation [19]:

$$J_n(x) \approx \sqrt{2/\pi}(x^2 - n^2)^{-1/4} \times \cos[(x^2 - n^2)^{1/2} - n \arccos(n/x) - \pi/4]. \tag{18}$$

It has been found that the values of  $n$  calculated with the use of expression (18) and the corresponding measured values for a sapphire DDR ( $\epsilon_1 \approx 11.5$ ,  $r_1 = 20$  mm,  $2b_1 = 0.98$  mm) [4] coincide to within their integers. Table 1 summarizes the calculated and experimental [4] values of azimuthal index  $n$  and WGM frequencies  $f$  (measurement error is  $\pm 0.01$  GHz) as well as the values of frequency intervals  $\Delta f$  between neighboring TE WGMs.

It is seen from the table that, at higher frequencies, the experimental values of WGM frequencies are closer to the calculated data. This circumstance is due to the fact that the slowing parameter of WGMs increases with frequency and, as a result, the concentration of the WGM energy inside the DDR grows. Therefore, the effect of the fields in the angular regions of the DDR on

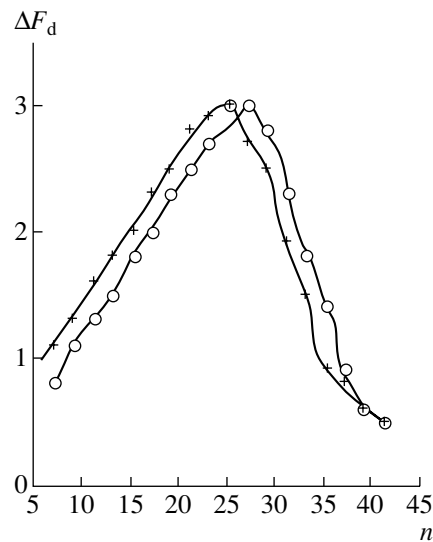


Fig. 5. Dependence of frequency intervals  $\Delta F_d$  between neighboring WGMs in a diamond DDR on  $n$ :  $t =$  (circles) 0.01 and (crosses) 0.10.

its DC is reduced. It should be noted that these fields are disregarded in the theory.

We have measured WGM frequencies in DDRs fabricated from compensated gallium phosphide (GaP;  $r_1 = 7$  mm,  $h = 1$  mm) and gallium arsenide (GaAs;  $r_1 = 5$  mm,  $h = 1$  mm). The measurements were performed in the band 80–120 GHz. The frequencies measured (with an error of  $\pm 0.02$  GHz) with a panoramic scalar network analyzer are summarized in Table 2.

The experimental data presented in Tables 1 and 2 confirm the presence of a maximum in the dependence of the rarefaction values of the WGM spectrum (frequency intervals  $\Delta f$  between neighboring WGMs) on large azimuthal indices  $n$ .

In order to find in a real situation the Q factor of WGMs in a DDR with known constitutive and geometric parameters, it is necessary to take into account that the intrinsic Q factor is limited by the radiation Q factor, which is determined by the radiation of a portion of the WGM energy into the open space. The radiation Q factor is rather high when  $r_1 > 10\lambda_0/\sqrt{\epsilon_1} \approx 20\pi/k_0\sqrt{\epsilon_1}$

Table 1

$n$ (Calculated)	22	23	24	25	26
$n$ (Experimental)	22	23	24	25	26
$f$ , GHz (Calculated)	32.11	32.92	33.75	34.65	35.42
$f$ , GHz (Experimental)	31.96	32.80	33.68	34.58	35.40
$\Delta f$ , GHz (Calculated)	–	0.81	0.83	0.90	0.79
$\Delta f$ , GHz (Experimental)	–	0.84	0.88	0.90	0.82

**Table 2**

GaP	$f$	80.32	82.27	84.30	91.48	93.49	95.59	101.12	103.17	105.20
	$\Delta f$	–	1.95	2.03	–	2.01	2.1	–	2.05	2.03
GaAs	$f$	80.47	82.64	84.84	86.77	89.00	93.07	95.31	102.19	104.35
	$\Delta f$	–	2.17	2.2	–	2.23	–	2.24	–	2.16

or  $k_0 r_1 \sqrt{\epsilon_1} > 60$  [16]. This relationship makes it possible to find the interval of operating frequencies where the radiation Q factor is substantially higher than the WGM intrinsic Q factor, which is determined by the dielectric loss in the material of a DDR.

Below, we present estimated radiation Q factors  $Q_r^{\text{TE}}$  of TE modes for certain specific cases [5]. These estimates have been obtained at  $f = 100$  GHz. The results are as follows: For a diamond DDR ( $\epsilon_1 = 5.7$ ) of the height  $h = 0.7$  mm,  $Q_r^{\text{TE}} \approx 10^7$  and  $2 \times 10^4$  at  $r_1 = 12$  and 8 mm, respectively, and, for a silicon DDR ( $\epsilon = 11.6$ ) of the height  $h = 0.5$  mm,  $Q_r^{\text{TE}} \approx 10^9$  at  $r_1 = 5$  mm. Numerical estimation of  $Q_r^{\text{TE}}$  for a leucosapphire DDR ( $\epsilon \approx \epsilon_{\parallel} = 11.5$ ,  $R = 20$  mm,  $h = 0.98$  mm) performed at 31 GHz ( $n = 20$ ) yields the value  $Q_r^{\text{TE}} \approx 10^{16}$ , while the Q factors measured in [4] at the same frequency range within the interval  $\approx (1.6-1.8) \times 10^5$ . The calculated radiation Q factor substantially exceeds the measured value. Therefore, the latter characterizes the dielectric loss in the resonator's material.

It is seen from the above estimates that the radiation Q factor abruptly increases as the DDR's radius and permittivity grow.

## CONCLUSIONS

The EP method for solution of the dispersion problem of WGM propagation in DDRs has been improved. The ratios of external wave numbers to internal wave numbers have been used as dimensionless parameters. With these parameters, the DEs for an infinite dielectric cylinder have been simplified and a rigorous numerical calculation has been performed in order to solve the vector problem for hybrid WGMs in the cylinder at large azimuthal indexes  $n$ .

The substantial effect of the small height-to-radius ratio of a DDR on the dispersion and spectral characteristics of WGMs has been revealed.

The calculated frequencies and azimuthal indices of WGMs in DDRs fabricated from various materials correspond to the experimental data.

The theoretical and experimental investigations have revealed the presence of a maximum in the dependence of frequency intervals between neighboring WGMs in a DDR on the large azimuthal indices. This result makes it possible to optimize the geometric dimensions of thin DDRs with relatively large radii and high radiation Q factors in a given frequency range within which high Q factors of DDRs are measured. In particular, such an optimization can be performed in the case when low dielectric losses are measured by means of the DDR method.

## ACKNOWLEDGMENTS

This study was supported in part by INTAS, project no. 01-2173, and by the Russian Foundation for Basic Research, project no. 03-02-16257.

## REFERENCES

1. L. V. Alekseichik, L. I. Brodulenko, V. M. Gevorkyan, et al., *Obz. Elektron. Tekh., Ser. 1: Elektron. SVCh (Moscow)*, No. 13(382), 1 (1981).
2. V. B. Braginskii, V. I. Panov, and A. V. Timashov, *Dokl. Akad. Nauk SSSR* **267** (1), 74 (1982).
3. J. Krupka, K. Derzakowski, A. Abramowich, et al., *IEEE Trans. Microwave Theory Tech.* **47**, 752 (1999).
4. V. N. Derkach, A. V. Golick, A. A. Vertij, et al., in *Physics and Engineering of Millimeter and Sub-Millimeter Waves (Proc. 4th Int. Symp., Kharkov, Ukraine, June 4-9, 2001)* (IRE NASU, Kharkov, 2001), p. 823.
5. V. B. Braginskii and S. P. Vyatchanin, *Dokl. Akad. Nauk SSSR* **252**, 584 (1980).
6. G. Annino, M. Gassetari, I. Longo, and M. Martinelli, *IEEE Trans. Microwave Theory Tech.* **45**, 2025 (1997).
7. V. V. Shevchenko, *Izv. Vyssh. Uchebn. Zaved., Radiofiz.* **14**, 768 (1971).
8. V. S. Dobromyslov and V. F. Vzyatyshev, *Trudy MEI: Radiotekhnika*, No. 161, 78 (1973).
9. B. M. Garin, V. P. Mal'tsev, and B. A. Murmuzhev, in *Physics and Application of Microwave (Tr. IX All-Russ. School-Seminar, Zvenigorod, Mosc. Region, May 26-30,*

- 2003) (Mos. Gos. Univ., Moscow, 2003), Part 1, p. 46 [in Russian].
10. V. S. Dobromyslov, M. Sh. Antipova, and S. D. Yakukhin, *Trudy MEI*, No. 194, 74 (1974).
  11. K. N. Tsibizov, S. A. Borisov, and Yu. M. Bezborodov, *Zarubezh. Radioelektron.*, No. 11, 21 (1981).
  12. C. Vedrenel and I. Arnaud, *Proc. IEE* **129** (4), 183 (1982).
  13. M. E. Il'chenko, *Dielectric Resonators* (Nauka, Moscow, 1987) [in Russian].
  14. R. M. Knox, *IEEE Trans. Microwave Theory Tech.* **24**, 806 (1976).
  15. D. Hondros and P. Debye, *Ann. der Phys.* **32**, 465 (1910).
  16. V. F. Vzyatyshev, *Dielectric Waveguides* (Sovetskoe Radio, Moscow, 1970) [in Russian].
  17. B. Z. Katsenelenbaum, *High-Frequency Electromagnetics* (Nauka, Moscow, 1966) [in Russian].
  18. E. Jahnke, F. Emde, and F. Lösch, *Tables of Functions, with Formulae and Curves* (McGraw-Hill, New York, 1960; Nauka, Moscow, 1977).
  19. H. Hönl, A. W. Maue, and K. Westpfahl, *Handbuch der Physik*, Ed. by S. Flügge (Springer, Berlin, 1961; Mir, Moscow, 1964), vol. 25/1, p. 218.